The Meteoritical Society

Meteoritics & Planetary Science 42, Nr 7/8, 1373–1386 (2007)
Abstract available online at http://meteoritics.org

Coordinated isotopic and mineralogic analyses of planetary materials enabled by in situ lift-out with a focused ion beam scanning electron microscope

Thomas J. ZEGA[1*], Larry R. NITTLER[2], Henner BUSEMANN[2†], Peter HOPPE[3], and Rhonda M. STROUD[1]

[1]Materials Science and Technology Division, Naval Research Laboratory, 4555 Overlook Avenue SW, Washington, D.C., 20375, USA
[2]Department of Terrestrial Magnetism, Carnegie Institution of Washington, 5241 Broad Branch Road NW, Washington, D.C., 20015, USA
[3]Max Planck Institute for Chemistry, P.O. Box 3060, 55020 Mainz, Germany
[†]Present address: Planetary and Space Sciences Institute, The Open University, Walton Hall, Milton Keynes, MK7 6AA UK
[*]Corresponding author. E-mail: zega@nrl.navy.mil

(Received 12 October 2006; revision accepted 22 April 2007)

Abstract–We describe a focused ion beam scanning electron microscope (FIB-SEM) technique that enables coordinated isotopic and mineralogic analysis of planetary materials. We show that site-specific electron-transparent sections can be created and extracted in situ using a microtweezer and demonstrate that they are amenable to analysis by secondary ion mass spectrometry (SIMS), scanning electron microscopy (SEM), and transmission electron microscopy (TEM). These methods greatly advance the ability to address several fundamental questions in meteoritics, such as accretion and alteration histories of chondrules and the origin and history of preserved nebular and presolar materials.

INTRODUCTION

Primitive meteorites, interplanetary dust particles (IDPs), presolar grains, and the newly returned Stardust samples from the Wild-2 comet are bountiful sources of information about the chemical and physical processes that shaped our solar system and galaxy. The information acquired from such materials can be maximized by performing coordinated analytical studies on them. For example, meteorites and IDPs contain submicron to micron-sized grains with unusual isotopic compositions, indicating that they condensed in the outflows of prior generations of stars (e.g., Nittler 2003). In correlated structure-isotope studies of presolar stardust grains, isotopic compositions (determined by mass spectrometry) can reveal the particular class, size, and metallicity of the star in which a given submicron-sized grain originated (e.g., Nittler 2003), and transmission electron microscope (TEM) analysis of the grain microstructure can constrain the pressure, temperature, and cooling rate of the stellar outflow (Bernatowicz et al. 2005; Croat et al. 2005). Also observed in the most primitive extraterrestrial materials are spatially concentrated enrichments of deuterium (D) and ^{15}N, relative to terrestrial D/H and ^{15}N/^{14}N ratios, believed to indicate partial preservation of organic matter that formed in interstellar space before solar system formation (Messenger 2000; Busemann et al. 2006a). Coordinated analysis of this anomalous material by TEM, synchrotron X-ray, and infrared techniques provides valuable information about its chemical nature, origin, evolution, and relationships to surrounding meteoritic material (Keller et al. 2004; Floss et al. 2004).

Performing coordinated studies of submicron, rare, or one-of-a-kind material is a challenging experimental task. In general, the specific region of interest (ROI) needs to be isolated from its surrounding matrix for detailed analysis, and, for TEM study, thinned to electron transparency. Such transparency is generally achieved by reducing the thickness of the sample to ≤100 nm in the direction of the electron beam. However, conventional sample-preparation techniques such as ion-milling or microtoming (reviewed by Barber 1999) are problematic because they lack the site specificity typically required for preparation of submicron grains and also because of the potential for alteration of petrographic information by differential ion milling or chattering during microtome slicing. The development of the focused ion beam (FIB) workstation and ex situ lift-out techniques was an important advance for coordinated analyses because they enabled site-specific extraction of micron- to submicron-sized features. In the ex situ lift-out technique, electron-transparent membranes are prepared using a focused Ga^+ ion beam and then removed from the focused ion beam (FIB) and transferred, under an optical microscope, to a TEM support film (e.g., Gianuzzi et al. 1997). This technique has been applied to a range of earth and planetary materials including presolar grains, primitive meteorites, and terrestrial minerals

(Heaney et al. 2001; Dobrzhinetskaya et al. 2003; Lee et al. 2003; Seydoux-Guillaume et al. 2003; Wirth 2004; Stroud et al. 2004a; Benzerara et al. 2005).

While ex situ lift-out overcame the site-specific limitation of ion milling, the continuous amorphous films on which the sections are supported (typically C or SiO) present potential problems. For example, supporting the section by such films precludes compositional analysis of elements in common with them. In the case of planetary materials, use of either film composition presents obvious difficulties if one wants to investigate the relationship between silicates and organics (e.g., Zega et al. 2006b). Also, the films are susceptible to penetration by the glass needle typically used to perform ex situ transfer of the FIB section, which can lead to a total loss of the sample. Further, the support film adds to the total thickness of material through which the interrogating radiation must propagate, which, in the case of the TEM, can lead to the blurring of image features. Films with holes in them, i.e., so-called holey films, might seem to offer an alternative means of support because they do permit transmission of the electron beam exclusively through the sample, thus eliminating the film's contribution to acquired TEM data. However, the micromanipulation of the ex situ method lacks the precision to ensure exact placement of micron to nanoscale ROIs over a hole in the film. Moreover, even if ex situ lift-out were capable of such precision, the support film could still interfere with coordinated analyses by methods other than TEM, e.g., secondary ion mass spectrometry (SIMS).

The development of combination FIB and scanning electron microscope (SEM) instruments (FIB-SEM) with in situ micromanipulators rectifies the problems of ex situ lift-out. The FIB-SEM combines all of the nondestructive imaging and analytical capabilities of the modern field-emission SEM with the sputtering capabilities of an ion beam 10 nm in diameter (e.g., Giannuzzi and Stevie 2005). Further, the ion beam can be used to customize the shape of a micromanipulator (herein, a microtweezer) that supports the sample, thus eliminating the need for a support film, and is adaptable to a wide variety of analysis geometries. Here we describe the microtweezer approach to in situ sample extraction and provide examples that demonstrate the power of the technique for addressing fundamental questions in planetary materials research.

EXPERIMENTAL METHODS

Electron-transparent sections of extraterrestrial materials were created at the Naval Research Laboratory (NRL) using an FEI Nova 600 FIB-SEM microscope equipped with an Ascend Instruments Extreme Access lift-out tool. The Nova 600 utilizes a Ga^+-ion gun and an electron gun at a 52° angular separation, enabling simultaneous milling and imaging. We analyzed the electron-transparent sections at NRL using a 200 keV JEOL 2200FS TEM equipped with bright-field and high-angle annular-dark-field STEM detectors, an in-column energy filter, and an energy-dispersive spectrometer. Some samples were analyzed with a JEOL 6500F thermally assisted field-emission SEM, equipped with an EDAX EDS system, at the Carnegie Institution of Washington. SIMS was performed using Cameca IMS 6f and NanoSIMS 50 ion probes at the Carnegie Institution of Washington and Max Planck Institute for Chemistry, Mainz, respectively.

DESCRIPTION OF THE TECHNIQUE

Creating an electron-transparent section can be divided into three steps: coarse cutting, in situ extraction, and in situ thinning. Coarse cutting is similar to that discussed in Heaney et al. (2001), Lee et al. (2003), and Wirth (2004), and so we provide only a brief description of it here. First, a ROI from which the section will be created is chosen (Fig. 1a). The sample is then tilted 52° to bring its surface perpendicular to the ion gun. A thin band of Pt, referred to as a strap, is deposited over the ROI (Fig. 1b) and serves to protect the underlying material from radiation damage and implantation of Ga^+ ions during the sputtering process. We note that sample-charging effects, if any, can generally be minimized by depositing a conductive coating on top of the sample (e.g., Au or C), or by extending a piece of conductive material (e.g., Cu or C) from the sample surface to its support. A section is then created by removing material from either side of the Pt strap (Fig. 1c). Several patterns can be used, but a rectangular shape with a stair-step profile is most efficient because it removes an amount of material sufficient to access the section while preventing it from falling down into the hole in the event that it cleaves from the substrate prior to lift-out. A rectangular pattern is then defined to thin the section to a 0.5 to 2 μm thickness (Figs. 1c and 1d). If ex situ lift-out was being performed, thinning would continue to approximately 100 nm. However, for the in situ method we discuss here, the final thinning is performed in situ after the section is extracted from the substrate (described below). In final preparation for in situ extraction, the sides of the section are then removed, leaving only the bottom attached to the substrate. The stage is then tilted back to 0°, the coordinates for the position of the section are stored, and it is removed from the field of view using the stage-translation controls.

Extraction of the section is performed using micrometer-sized tweezers (microtweezers) that are fabricated out of the tip of the support grid, sold by Ascend Instruments LLC under the commercial name End-Effector (EE). The support grids are available in either Cu or Mo and consist of a horseshoe-shaped base approximately 3 mm across that tapers to a point and contains a slot hinge for post-extraction folding (Fig. 2a) into a geometry compatible with a TEM sample holder. The EE, held within a carrier that is secured to

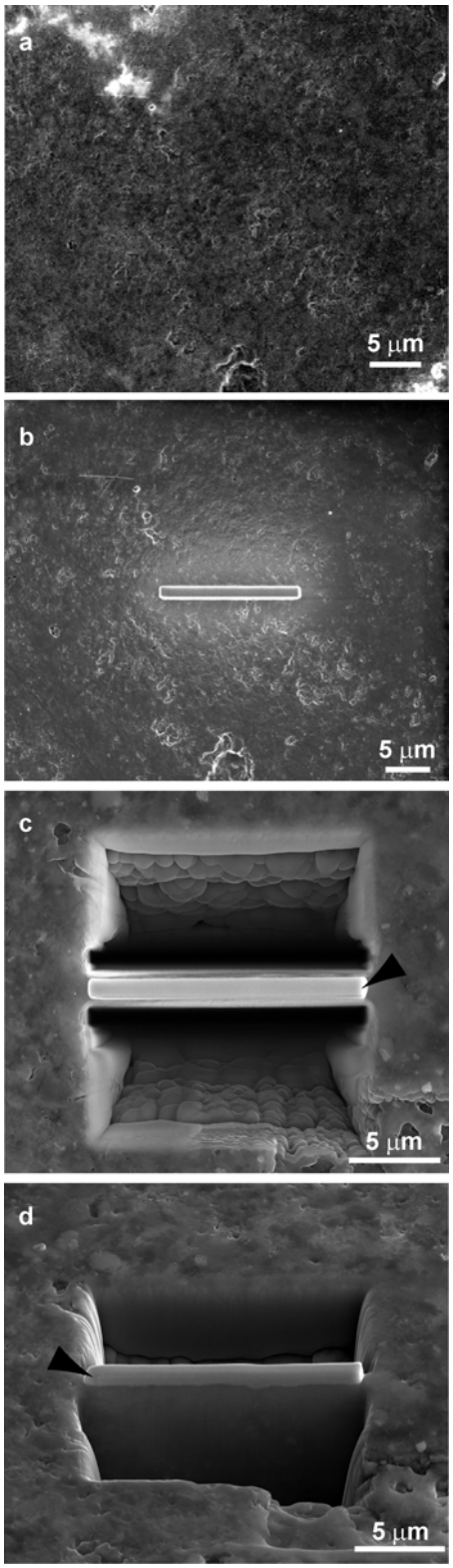

Fig. 1. Secondary electron images (SEIs) of an ROI from the Murray CM chondrite. a) Prior to and (b) after deposition of a Pt strap, which measures 15 μm wide × 1 μm high × 1 μm thick. c) After milling the material above and below the Pt strap (arrowhead). d) 52° oblique view of (c).

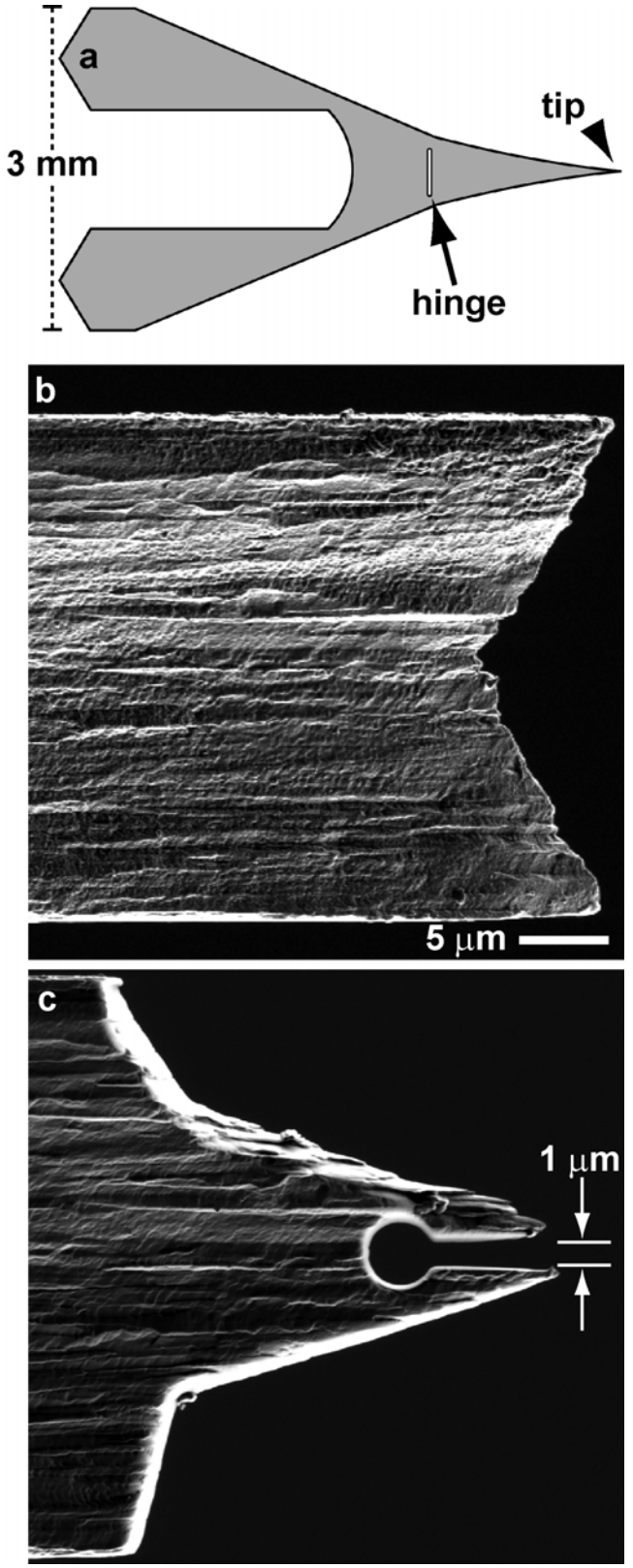

Fig. 2. End effector used to extract the section. a) Plan-view schematic. Edge-on SEI of the (b) raw tip and (c) microtweezer patterned from (b).

a sample rod, is rotated into edge-on orientation (using motor-drive controls) relative to the ion beam (Fig. 2b), and the ion beam is used to fabricate microtweezers (Fig. 2c) out of the tip. A 20 nA Ga^+ current is used for coarse cutting the microtweezers, and a 1 to 3 nA current is used for cleaning rough edges. The microtweezers consist of a hole 2 to 3 μm in diameter centered between two prongs (Fig. 2c). The slot between the prongs is milled slightly narrower than the thickness of the section, and the hole permits the prongs of the microtweezers to expand around the section during capture.

To extract a sample, we capture the section with the microtweezer, detach it from the substrate, and lift it out (all coarse and fine manipulation of the microtweezer is performed using a combination of motor and piezo drives, respectively). First, the ROI is brought back into the field of view with the microtweezer safely out of the way so that it is not damaged during stage translation. While imaging with the electron beam, the microtweezer is then brought back into the field of view and its rotation is adjusted so that the plane of the slot between the prongs is parallel to the top and bottom surfaces of the section. The x and y position of the microtweezer is adjusted so that it sits above the ROI with the section appearing between the prongs of the microtweezer in projection (Fig. 3a). The microtweezer is then translated downward in order to slide the prongs over the top and bottom surfaces of the section. However, because the electron beam is oriented normal to the sample surface, it can be difficult to judge the distance between the bottom side of the microtweezer and the top of the section. Thus, the oblique view provided by the ion beam (52° from normal incidence or 38° from the sample surface) gives the best indication of this distance and shows that the prongs of the microtweezer are several micrometers above the section (Fig. 3b). Iterative translation and image acquisition is the best way to gauge the proximity of the microtweezer to the section, but extended viewing with the ion beam is avoided to limit ion implantation and radiation damage. Once the microtweezer contacts the section, indicated by a change in the contrast of the secondary electron image (SEI), the microtweezer is lowered further so that the prongs expand (in response to the applied stress) to accommodate the thickness of the section (Fig. 3c). The section is secured in the microtweezer by the tensional force imparted on it by the prongs, and so the depth to which the microtweezer is lowered (Fig. 3d) is important and depends on several factors, including the size and location of the ROI. It is desirable to obtain the strongest possible grip on the section while minimizing the amount of surface area that is obscured by the prongs of the microtweezers. As an added measure of security, although generally not needed, the ion beam can be used to weld the microtweezer and FIB section together by depositing a small amount of Pt overlapping both. Once the microtweezer is securely fastened, it is necessary to detach the section from the substrate so that it can be lifted out of the hole. A rectangular pattern 1 μm wide is defined at the base of the section (using the FIB software), and the ion beam is used to mill away the material within it (Figs. 3e and 3f). The microtweezer is then translated upward to lift the section out of the hole and into a safe position away from the sample surface (Figs. 3g and 3h). The stage is then moved out of the field of view so that material is not sputtered onto the sample surface during in situ thinning.

The sample as lifted out can be thinned to electron transparency (~100 nm) or left as is, depending on the type of analysis to be performed. For in situ thinning, the section must be rotated so that the Pt strap faces the ion gun and protects the material beneath from Ga^+ ion implantation and radiation damage (Fig. 4a). The ion beam is then used to thin the part of the section that is suspended beyond the prongs of the microtweezer (Fig. 4b). Rectangular patterns are used to iteratively thin the section to the desired thickness. Short milling times between successive milling cycles are preferred to ensure minimal sample drift. With careful monitoring of the thinning process and detailed measuring of images acquired after each milling cycle, thicknesses of ≤100 nm can routinely be achieved (Fig. 4c). The section is approximately 1.5 μm thick where it is held between the prongs of the microtweezer (Figs. 4b and 4c) and 100 nm thick where it is cantilevered beyond the prongs and suspended in free space (Figs. 4c and 4d). The sample rod is then removed from the FIB-SEM microscope and inserted into a mechanical device in which the microtweezer with sample attached (Fig. 5a) is folded 180° onto itself (Fig. 5b) to fit directly into the TEM sample holder.

EXAMPLE APPLICATIONS OF THE LIFT-OUT TECHNIQUE

Here we describe some examples of applying the in situ lift-out technique to planetary materials. We note that our purpose is not to exhaustively discuss the scientific ramifications of the results, but rather to illustrate the power of the lift-out technique for a range of important problems in meteoritics. Detailed scientific discussions of the various examples will be deferred to dedicated papers on the specific subjects.

Matrix and Chondrule-Rim Sections

Among the most actively researched topics in meteoritics are the origins of chondrules and calcium-aluminum-rich inclusions (CAIs), and associated fine-grained rims (FGRs) and their relationship to matrix materials (e.g., MacPherson et al. 1988; Metzler et al. 1992; Buseck and Hua 1993; Hewins 1997). A major obstacle to these studies has been the difficulty in preparing electron-transparent sections that span the chondrules, CAIs, FGRs, and matrix components (e.g., Zega and Buseck 2003). The differential thinning of micrometer-

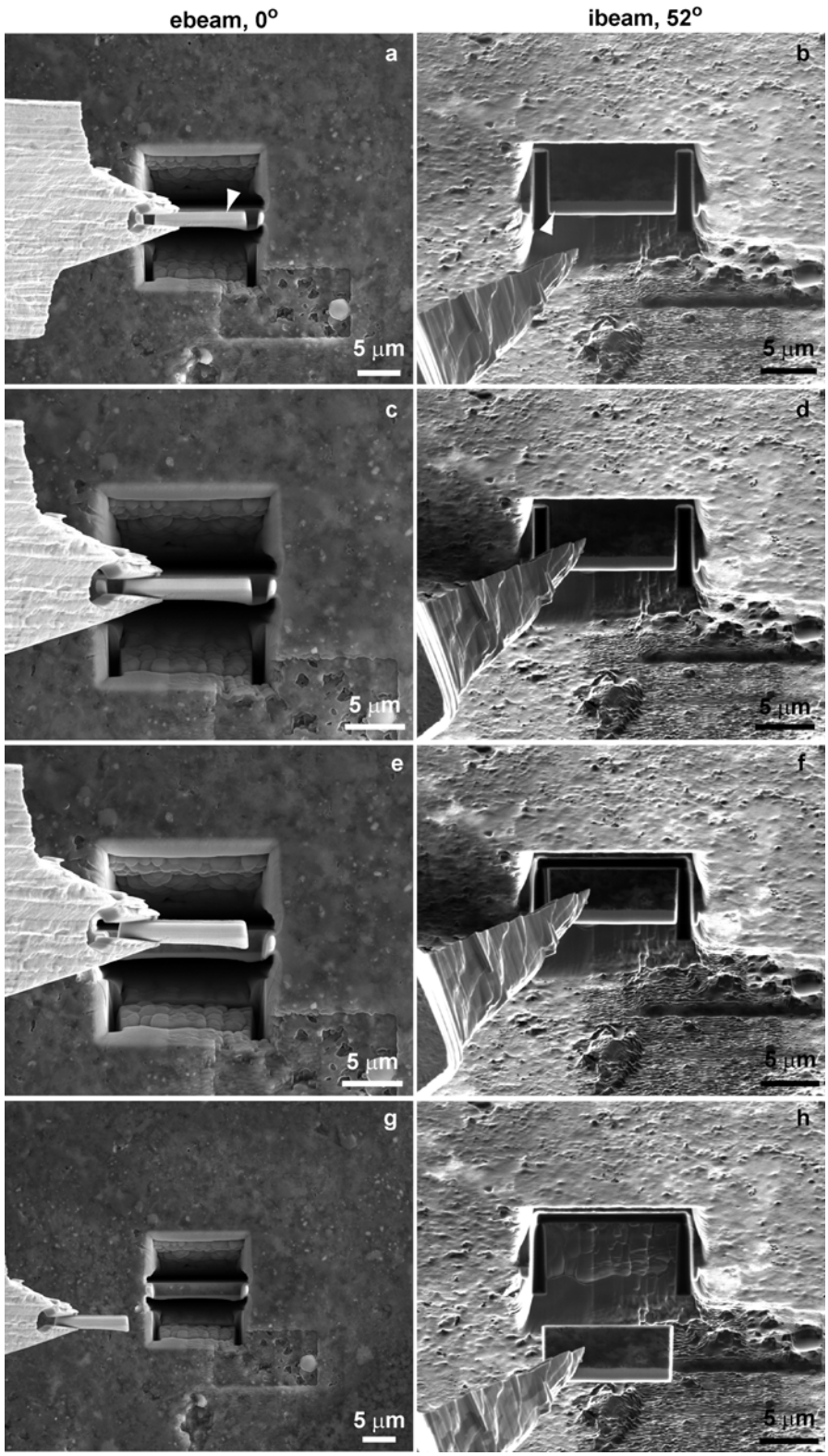

Fig. 3. SEIs of the lift-out process. a) Alignment of the prongs of the microtweezer with the section. The plane of the slot between the prongs is parallel to the top and bottom surfaces of the section. b) Oblique view of (a). White arrowheads point to the Pt strap. c) Microtweezer lowered onto the section. d) Oblique view of (c). e) Undercutting of the section. f) Oblique view of (e). g) Section lifted out of the hole and moved to a position safely above the sample surface. h) Oblique view of (g). The rectangular region off the lower right corner of the bottom trench is eroded because that is where focus and astigmatism were intermittently adjusted using a reduced raster.

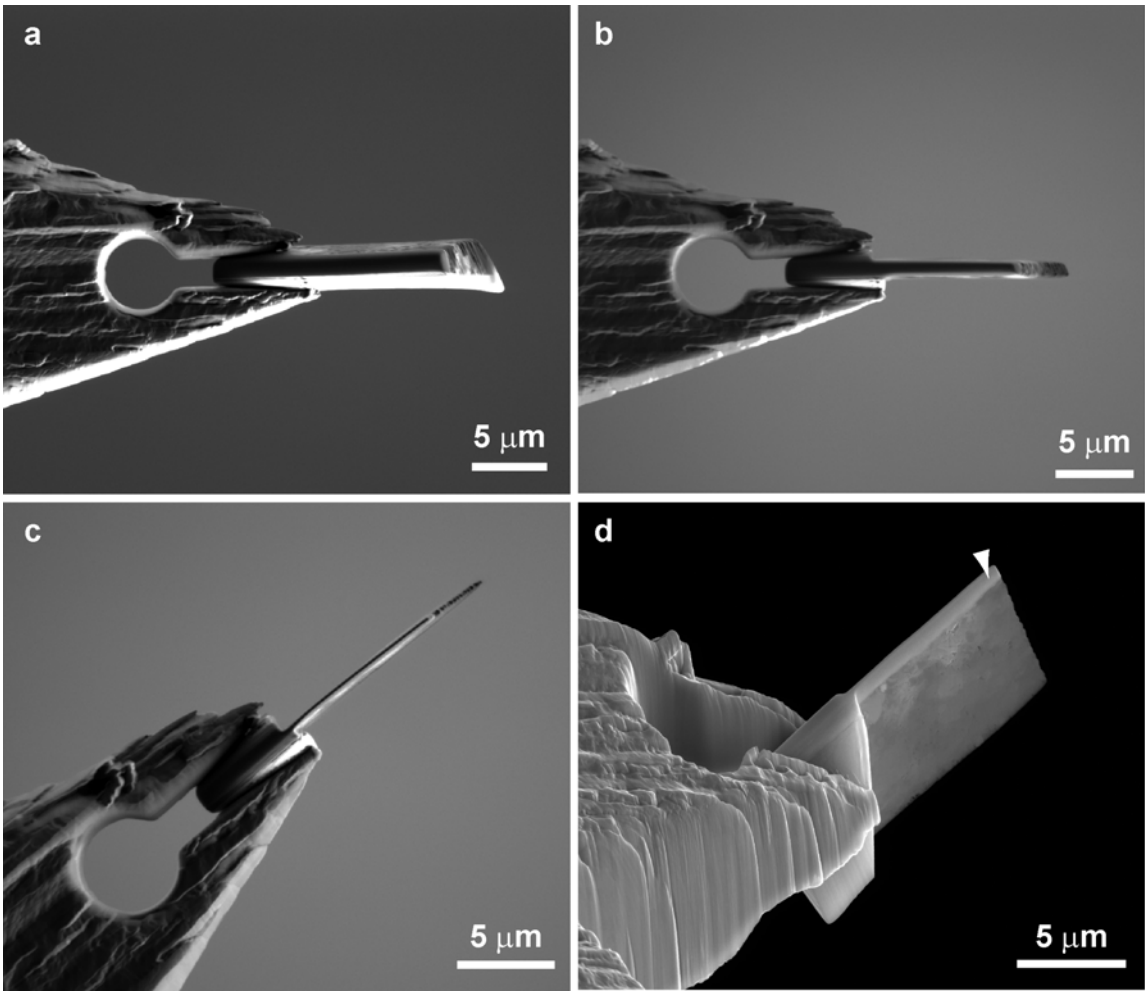

Fig. 4. SEIs of the in situ thinning process. a) As-lifted-out 2 μm thick section. b) 500 nm thick section. c) 100 nm thick section. d) End effector rotated clockwise from (c). Pt strap indicated by the white arrowhead.

sized compared to nanometer-sized grains, and refractory oxides and silicates compared to metals, sulfides, phyllosilicates, and organics results in selective loss of the finer and softer materials, which can produce thin areas with non-representative mineralogy. The geometry of the FIB-SEM method, in which the ion beam is normal to the ROI rather than the 10 to 20° used for broad-beam ion milling, along with the in situ imaging capabilities, surmounts this problem.

As an example of the application to chondrule studies, we extracted a section that transects a chondrule-FGR boundary from a petrographic thin section of the Murray carbonaceous chondrite (Fig. 6a). The 1 μm thick protective layer of Pt that was deposited onto the surface of the ROI prior to milling (Fig. 6b) appears as a bright band at the top of the section in the SEI (Fig. 6c) and the high-angle annular-dark-field (HAADF) image (Fig.7a). The as-lifted-out, ~2 μm thick area of the section also appears bright in the HAADF image but contains a region of dark contrast that corresponds to one of the prongs of the microtweezer (Fig. 7a, black arrowhead). A knife edge occurs across the chondrule where the 2 μm thick part of the section meets the 100 nm thick electron-transparent region (Fig. 7a, dashed white arrow) and extends from the base to the top of the section at a 73° angle (due to the angle of incident ions used to mill the section). The 2 μm thickness of the as-extracted region is relatively opaque to electrons. In comparison, the region thinned in situ to 100 nm is transparent to electrons and reveals areas with bright and dark contrast, which is indicative of material with high and low atomic number, respectively.

EDS shows that the part of the chondrule that is in contact with the FGR contains O, Mg, Si, and Fe with minor Al, Ca, Cr, and Ni (Fig. 7b), and quantification yields 1.2 and 3.0 for ratios of (Mg + Ca + Cr + Fe + Ni)/(Si + Al) and O/Si, respectively. Measurements on a selected-area electron-diffraction (SAED) pattern and high-resolution TEM (HRTEM) image from the chondrule grain (Fig. 7c) give 0.87, 0.64, and 0.93 nm *d*-spacings. The compositional and crystallographic data indicate that this part of the chondrule is composed of orthopyroxene. A 50 nm wide band occurs at the edge of the chondrule grain (Fig. 7d, white arrowhead) and

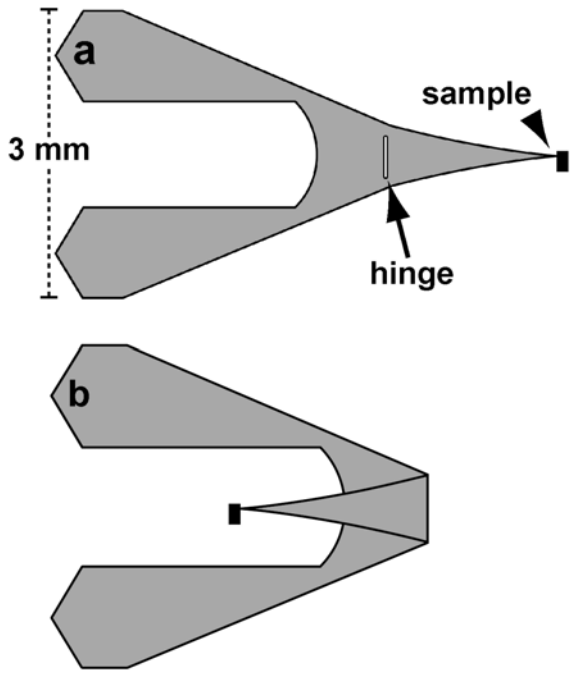

Fig. 5. Plan-view schematics of the EE. a) As removed from the FIB-SEM with sample attached. b) After folding by 180° onto itself into a geometry compatible with a TEM sample holder.

extends along its entire length. EDS mapping indicates that the band is rich in Fe (Fig. 7e). A region of material exhibiting dark contrast and variable thickness (~800 nm wide at the thickest part; 200 nm at the thinnest) occurs between the chondrule and FGR (Fig. 7d, black arrowhead with white outline). EDS shows that the material contains C, O, Mg, Si, Fe, with minor Al, Ca, Cr, and Ni, and SAED patterns indicate that it is amorphous. The amorphous material extends 6 μm from the base of the section, where it contains a region rich in Fe (cf. dashed box in Figs. 7d and 7e), and is bordered on its side and top by Fe-rich sheet silicates (Fig. 7d, gray arrowheads with black outline), Fe-Ni sulfides (Fig. 7d, white arrowhead with black outline), and a clast containing both of these mineral types (Fig. 7d, gray arrowhead).

The matrices and FGRs of CM-type carbonaceous chondrites sustained aqueous alteration early in their histories (Zolensky and McSween 1988; Buseck and Hua 1993), and determining the mineralogy of these components is important for understanding the location, mechanisms, and conditions under which such alteration reactions occurred. The presence of sheet silicates and Fe-Ni sulfides throughout this Murray FGR (Fig. 7d) is consistent with previous observations (Zolensky et al. 1993; Brearley et al. 1999; Lauretta et al. 2000; Zega and Buseck 2003; Zega et al. 2003, 2004, 2006a) and indicates pervasive aqueous alteration. The clast that contains sheet silicates and Fe-Ni sulfides (Fig. 7d, black arrowhead) exhibits distinct boundaries with the rim material along its bottom and lower-right edges, suggesting that it is a brecciated fragment that

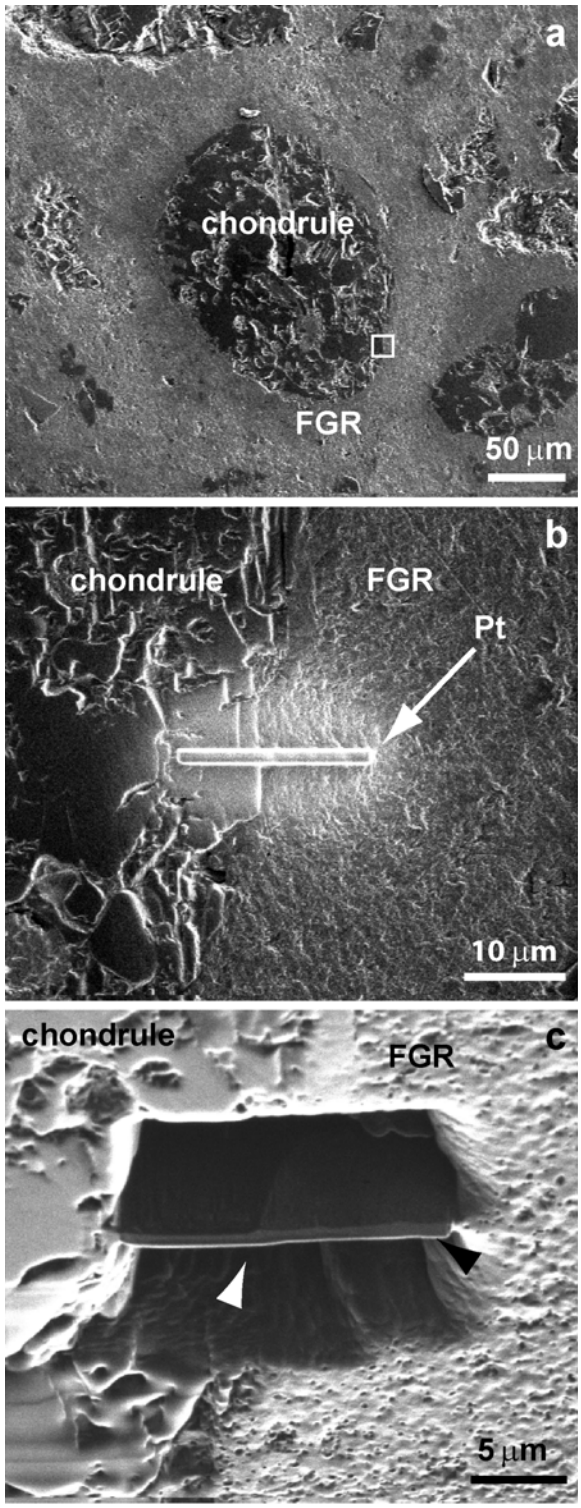

Fig. 6. SEIs of a chondrule-FGR assemblage from the Murray CM chondrite. a) Low-magnification image of the entire assemblage prior to Pt deposition. White box indicates the ROI to be extracted with the FIB-SEM. b) Higher-magnification image of the ROI after Pt deposition showing that the strap transects the chondrule-FGR interface. c) Oblique view of the FIB section as seen using the ion beam at 0° stage tilt. The Pt strap (black arrowhead) clearly transects the chondrule-FGR interface (white arrow).

accreted onto the chondrule with other FGR material. The lack of a discernible boundary along the top-right edge of the brecciated fragment is likely due to aqueous-alteration effects that produced the hydrated silicates within it. The edge of the chondrule exhibits a sharp boundary with the amorphous material but is less distinct at the top of the FIB section where hydrated silicates are abundant (Fig. 7d, top arrowhead) and appear to have overprinted part of the 50 nm wide band of Fe-bearing material. Taken together, the textural and compositional data are consistent with incipient alteration of the chondrule. Alteration probably took place on the parent body rather than in a nebular environment because gas-solid interactions, hypothesized as being characteristic of the latter (Fegley and Prinn 1989; Ciesla et al. 2003), would have likely resulted in uniform alteration of the chondrule. Extraction of additional sections from this chondrule-FGR boundary, which is possible with the in situ lift-out technique, could help determine whether the results are specific to this assemblage or are broadly applicable to the Murray CM chondrite.

Comparing the mineralogy of FGRs to that of their matrices is also useful for understanding the relationship of these components and deciphering the history of meteorites. Coordinated analyses on these kinds of samples is greatly facilitated by the in situ lift-out technique and thus a full complement of structural, compositional, and isotopic data can be obtained at the nanoscale. For example, we extracted a matrix section from the Murray CM chondrite, briefly analyzed it in the TEM (Fig. 8a), and then took it to the SEM where we acquired SEI and backscattered-electron images (BSE), and mapped the distribution of selected elements of the entire 7 × 16 micron section (spatial resolution <200 nm, integration time of 60 ms/pixel, total acquisition time of 13 min) using EDS (Figs. 8b–l). Following the SEM analysis, we used the NanoSIMS to also map the spatial distribution of selected isotopes (Figs. 8m–q). The electron images show that the section is well supported with the prong of the Mo microtweezer occluding the as-extracted 2 μm thick region (Figs. 8a–c, white arrowhead). The HAADF and BSE images show the Pt strap as a bright band, consistent with the Pt map (Fig. 8l). The distribution of Mo in the Mo L_α map (Fig. 8k) is consistent with the prong of the Mo microtweezer shown in the HAADF, BSE, and SEI images (Figs. 8a–c). The matrix has a heterogeneous composition as shown by the HAADF, BSE, EDS, and SIMS images. HAADF and HRTEM imaging reveal that hydrated material occurs in this FIB section of matrix, but the type, abundance, and distribution of this material differs from that in the FGR discussed above, suggesting possible variations in the degree of aqueous alteration on the parent body. We also note two correlations. C is concentrated near the Pt at the center of the section and at two spots on its right side (Fig. 8d). The ^{13}C tracks the ^{12}C, as expected, and there is no evidence for material with $^{13}C/^{12}C$ ratios distinctly different from the terrestrial value of ~0.011. Further, ^{14}N (measured as CN) correlates with ^{12}C near to the Pt and toward the right side of the section (cf. Figs. 8d, 8m, and 8p). O, Mg, and Si are concentrated at the base of the section (the side opposite the Pt), toward the right side, and correlate with a ~2 μm wide grain shown in both the HAADF and BSE images. We note that the SIMS and SEM-EDS maps for Si and O do not correlate well with one another. This most likely reflects instrumental effects, including both shadowing in the SEM, and matrix, secondary-ion focusing, and charging effects in the NanoSIMS. Additional coordinated SEM-SIMS analyses on FIB sections are needed to clarify these issues.

Presolar Grains and Organic Material

We demonstrated in the previous examples that isotopic and other measurements could be performed on the sections after the TEM analysis. However, the reverse situation also occurs in which an isotope study reveals a grain of primitive nebular or presolar origin, but additional structural and compositional data are required to determine the carrier of the isotopic anomaly. For example, lift-out methods can help address the origin and history of presolar grains and primitive organic materials in meteorites and interplanetary dust particles. We give two examples below.

The Tagish Lake carbonaceous chondrite was collected shortly after falling to Earth (Brown et al. 2000). It contains up to 3 wt% organic C (Grady et al. 2002), some of which contains enhanced D and ^{15}N (Busemann et al. 2006a). Using SIMS, we mapped the isotopic distribution of D and ^{15}N in matrix fragments of the Tagish Lake chondrite that were pressed into Au foil, an example of which is shown in Fig. 9 and discussed in detail by Busemann et al. (2006a). The matrix fragment (Fig. 9a) contains a D hotspot (~1 μm wide) in the upper-left region (Fig. 9b) that is enriched by 7000‰ relative to standard mean ocean water (SMOW). The D-rich region is also enriched in ^{15}N, with $\delta^{15}N$ = 400‰ (Busemann et al. 2006a). After SIMS analysis, we took the matrix fragment to the FIB-SEM, deposited a Pt strap that transects the D hotspot (Fig. 9c), and extracted a section for TEM analysis. A cross-sectional view of the section is shown in the mosaic of HAADF images (Fig. 9d). The material sandwiched between the Pt strap and the Au substrate exhibits dark and uniform contrast, consistent with a low-Z material that is rich in organic compounds. A detailed discussion of this section and several others we have extracted will be presented elsewhere.

Presolar grains are trace constituents of primitive chondrites and occur at ppm levels. Many types of presolar grains are acid insoluble and are concentrated by preparing acid-resistant residues of their parent meteorites (e.g., Amari et al. 1994). These residues are dispersed onto clean Au foils and analyzed by SIMS or other mass spectrometric techniques. Many presolar grains are easily identified by their

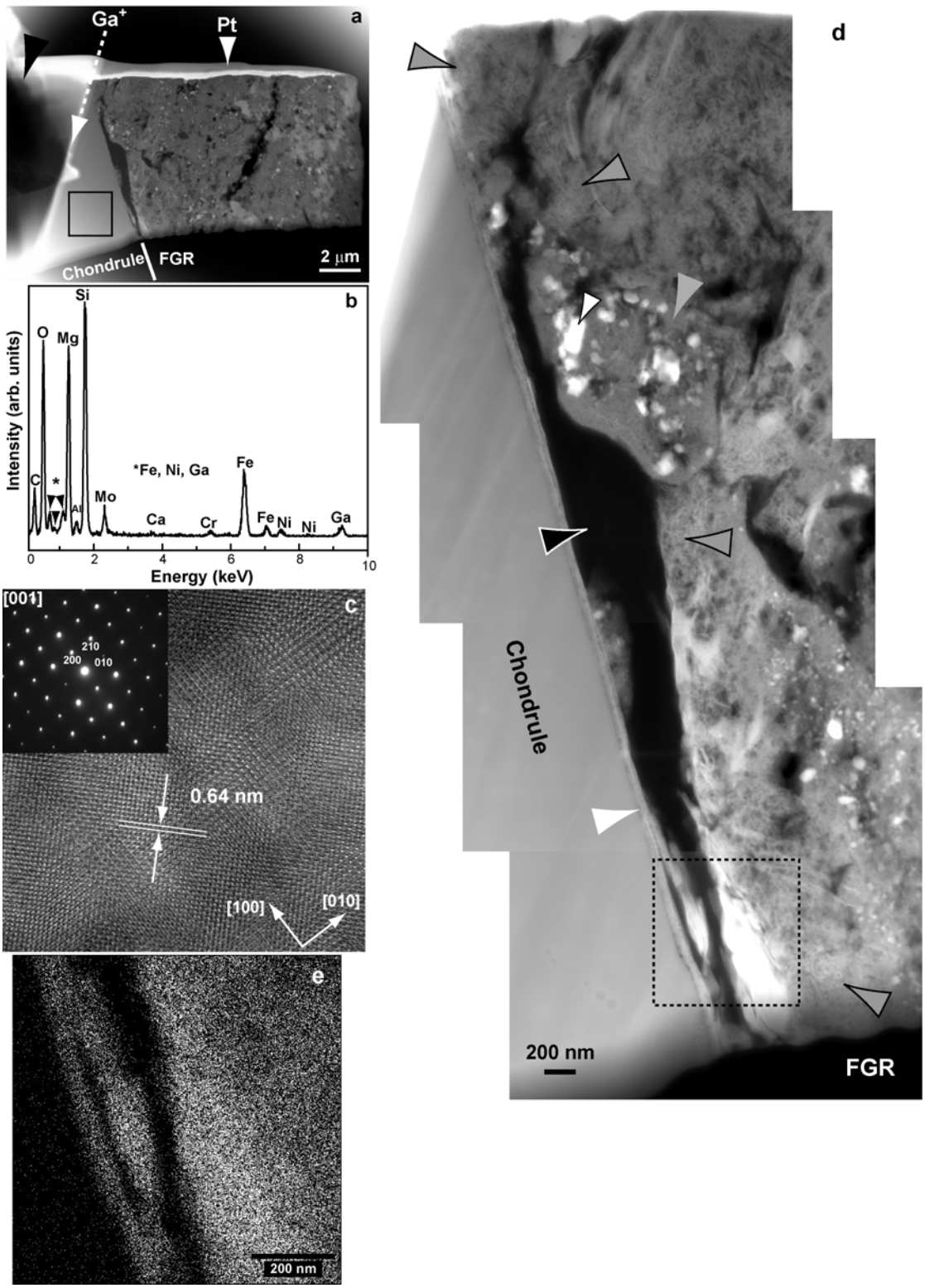

Fig. 7. TEM image and X-ray data of a chondrule-FGR assemblage from the Murray CM chondrite. a) HAADF images of the entire section showing the chondrule grain, FGR, the interface between them (solid white line), and prong of the microtweezer (black arrowhead). The path of the incident ions (white arrowhead with dashed line) used to thin the section is oriented at 73° relative to its base. b) EDS spectrum from the region in the chondrule outlined by the black rectangle. The Mo peak is from the microtweezer. c) HRTEM image of the chondrule. SAED pattern shown inset. d) HAADF image mosaic of the chondrule, FGR, and interface between them. Annotations are discussed in the text. e) Fe K_α X-ray map from the area outlined by the dashed black box in (d).

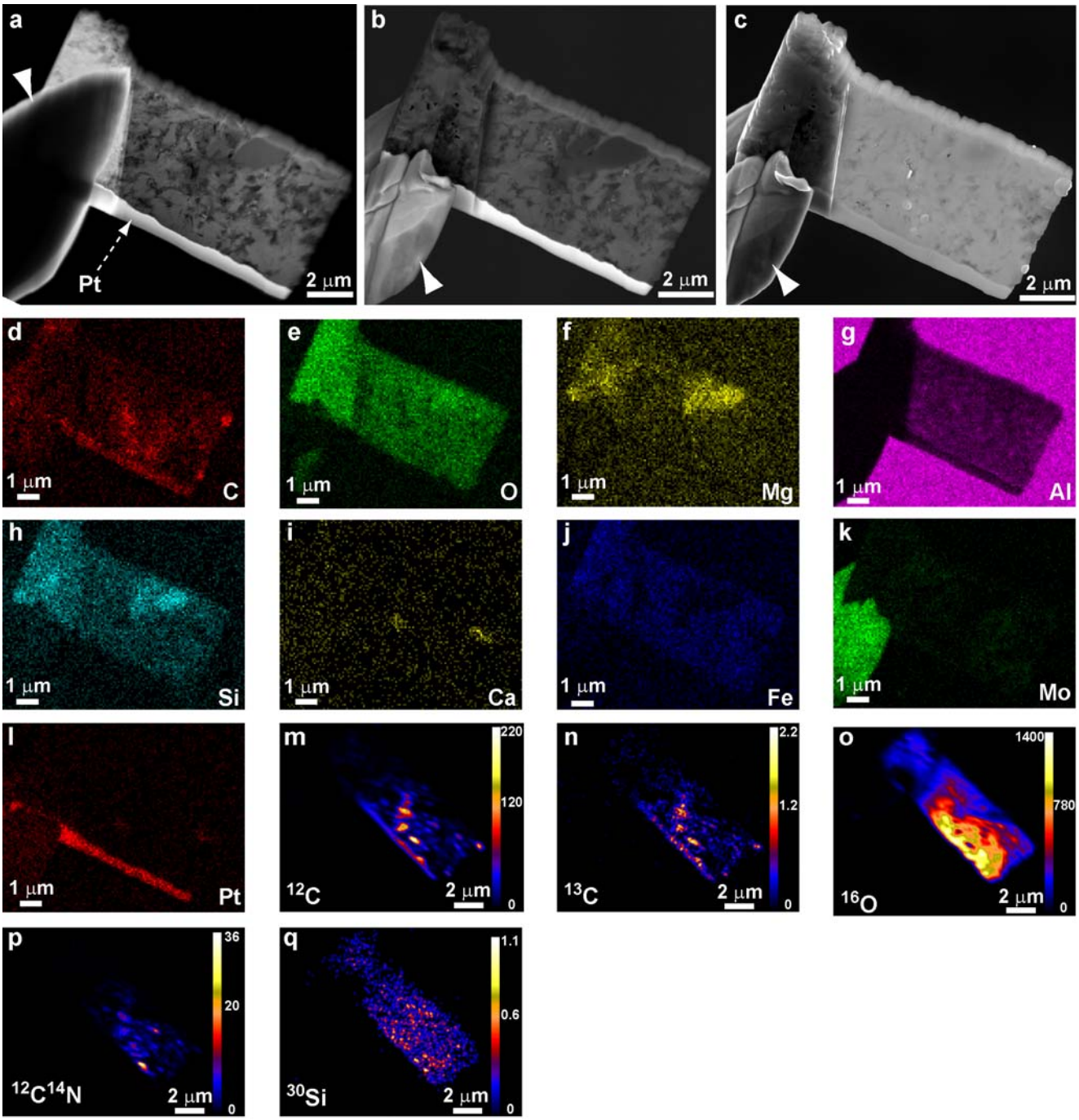

Fig. 8. Electron, X-ray, and isotope images of a matrix section from the Murray CM chondrite. a) TEM-HAADF image. b) SEM-BSE image. c) SEM-SEI image. d–l) X-ray maps of selected elements (indicated in the lower-right corner of each image). m–q) Maps of selected isotopes (indicated in lower left corner of each image). Images were acquired by rastering an ~100 nm Cs^+ beam over the sample with simultaneous collection of the secondary ions. Color correlates to the scale bar, which indicates the number of counts at each pixel.

extreme isotopic ratios in most elements, relative to materials that formed in the solar system. Even in acid-resistant residues, some types of presolar grains are rare, and automated SIMS techniques must be used to identify them among a larger number of less interesting grains (Nittler et al. 1997; Hoppe et al. 2000; Nittler and Alexander 2003). Once identified, presolar grains can be sectioned and lifted out (e.g., Fig. 10) for TEM analysis in essentially the same manner as used for petrographic thin sections. Moreover, following TEM analysis, these sections can be re-analyzed by NanoSIMS to directly correlate substructures with isotopic compositions. The use of ex situ and in situ lift-out has led to

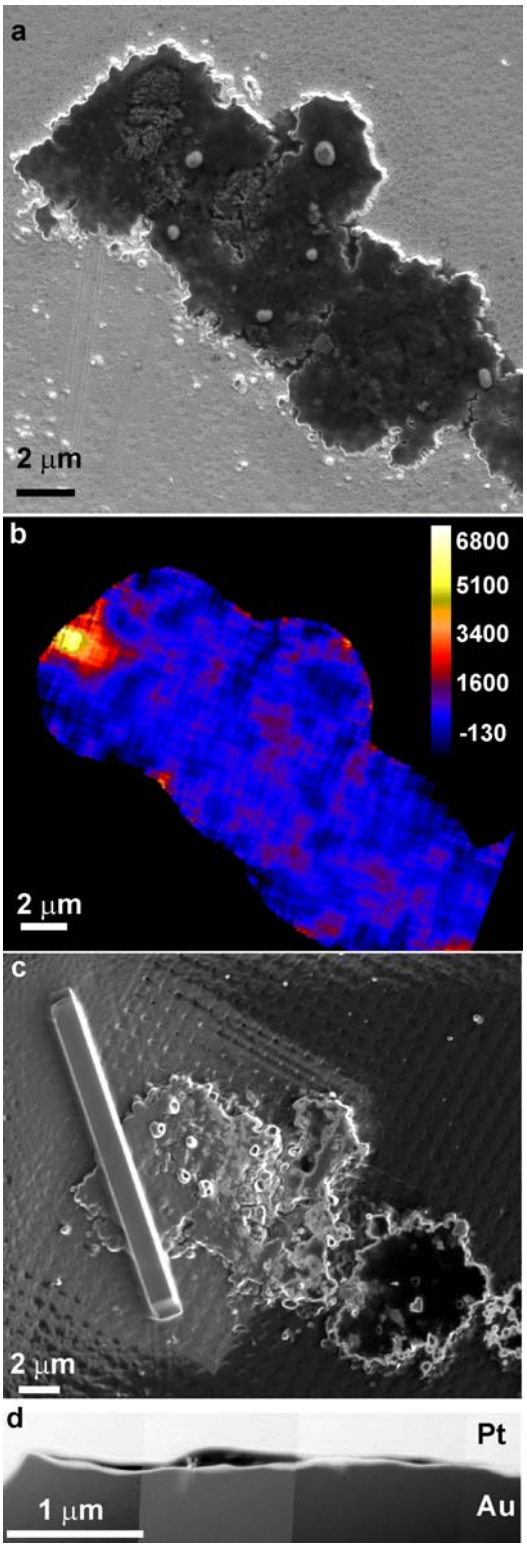

Fig. 9. Electron and isotope images of a matrix fragment of the Tagish Lake carbonaceous chondrite. a) SEI image of an ROI prior to mapping by SIMS. b) Map of D/H ratios given as per mil deviation from SMOW. Color correlates to the scale bar on the right. c) SEI image of the matrix fragment after deposition of the Pt strap. d) Cross-sectional HAADF image of the section after lift-out.

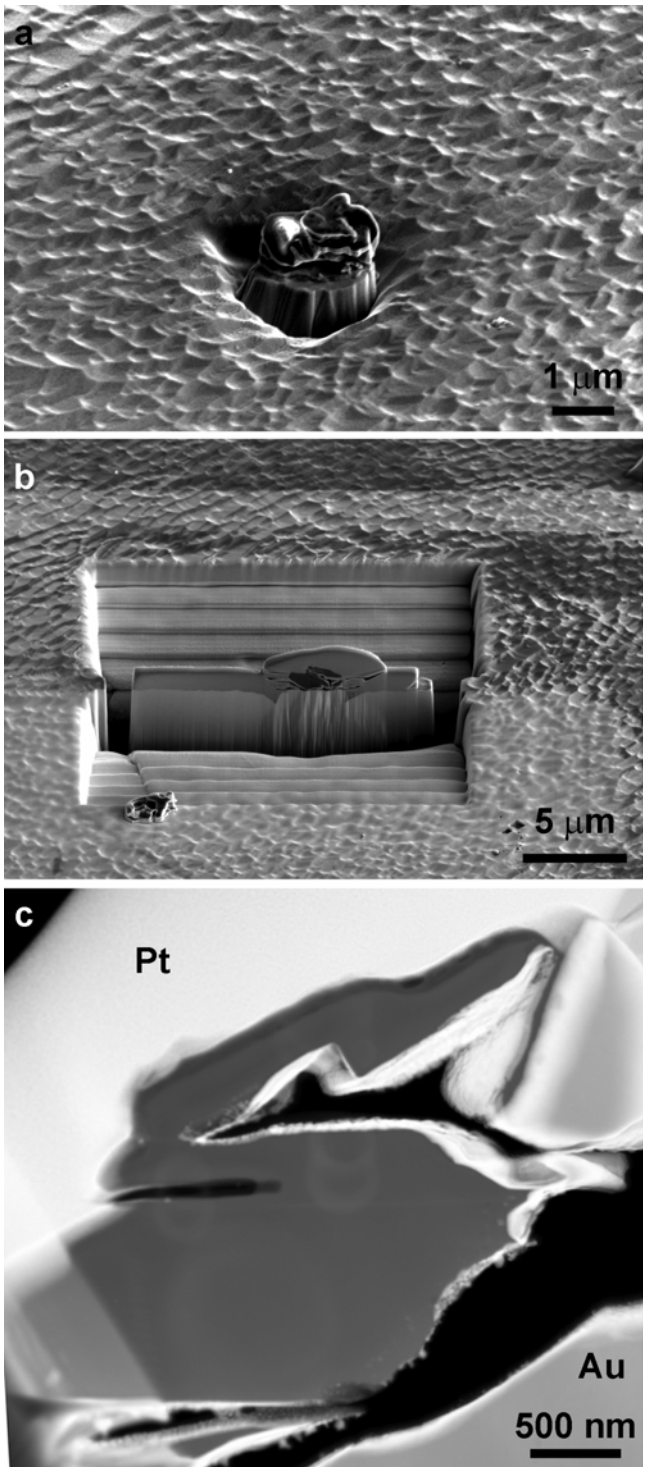

Fig. 10. Electron images of a presolar hibonite grain identified in an acid-resistant residue of the Krymka LL3.1 chondrite (Nittler et al. 2005). a) SEI of the grain on the Au-coated ion-probe mount after isotopic characterization. b) SEI (oblique view) of the Pt-coated section of the grain prior to extraction. c) Cross-sectional HAADF image of part of the section containing the hibonite grain sandwiched between the Pt and Au.

the first determinations of the structures of presolar Al_2O_3 (Stroud et al. 2004a), hibonite (Stroud et al. 2005), and supernova SiC (Stroud et al. 2004b) and Si_3N_4 grains (Stroud et al. 2006), providing insight into circumstellar dust-condensation processes and aiding the interpretation of stellar infrared spectra.

ADVANTAGES AND DISADVANTAGES

The major advantage of FIB is its orders-of-magnitude improvement in site specificity over Ar-ion milling, the more conventional ion-beam method of preparing electron-transparent samples. With the latter technique the nature of the sample support (typically a Cu washer with 3.0 mm outer diameter and variable inner diameter) necessarily consumes a large amount of material (hundreds of microns to mm) from, e.g., a petrographic thin section (see Zega and Buseck 2003 as an example), and the size of the Ar-ion beam (hundreds of microns in diameter at high angles; several millimeters at low angles) makes it challenging to target and thin sub-mm areas of interest for TEM analysis. In comparison, the 10 nm probe of the FIB provides unparalleled etching resolution, and combined with in situ lift-out, allows for far less material to be consumed (≤tens of μm).

FIB-SEM is not without certain difficulties and limitations. Like Ar-ion milling, FIB sectioning is an inherently destructive process, and ion implantation and structural damage are generally unavoidable (see Barber 1993 for a discussion of the damage effects of Ar-ion milling). The thickness of the amorphous layer and degree of ion implantation depends on several variables such as the target material and its bond strength, but both can generally be minimized by using low voltages (e.g., ≤5 kV) and currents (e.g., ≤0.1 nA) during the final stages of in situ thinning. Under low-dose conditions, amorphous layers and Ga concentrations in some of the planetary materials that we have experimented with were, respectively, less than 10 nm thick and below the detection limit of our EDS spectrometer. Although the thickness of the damage layer can be minimized, it is difficult to remove it completely without performing post-FIB processing such as plasma cleaning, reactive etching, or ion milling (e.g., Kato 2004; Ko et al. 2007). Thus, when performing in situ thinning, it is important to consider the thickness of the sample in terms of the ratio of damaged to undamaged material. Achieving thicknesses ≤50 nm is possible with the in situ method, and preferable for TEM analysis, but one must keep in mind that such a sample could potentially contain a 10 to 20 nm thick layer of damaged material on the top and bottom surfaces. Structural and compositional data acquired from such a sample might only come from 10 to 30 nm of undamaged material. We also note that re-deposition is not uncommon, but it too can be minimized using low-dose conditions during the final polishing step.

The preparation of a FIB sample can also be time consuming, generally requiring the operator to monitor the entire process. Although automating the coarse-cutting procedure is possible, it is best applied to samples for which the area of interest is large (mm) and homogeneous (such as bulk crystals) because sputtering rates are likely to be uniform and potential mishaps can be rectified by starting over on some other area of the sample. Automated FIB sectioning is thus unlikely to ever be widely implemented in planetary materials because of their uniqueness and heterogeneity. The different sputtering rates of, e.g., sheet silicates in a FGR and anhydrous silicates in chondrules can require additional milling time beyond that predicted from the calibrated sputtering rates of standard materials. In other words, a software package is unlikely to ever substitute for a user sitting at the workstation and judging if and when additional milling is necessary to produce a high-quality section. Regardless of whether or not the coarse-cutting process is automated, in situ lift-out and thinning absolutely require hands-on operation. Thus, it is our experience that most planetary samples require, on average, four to eight hours of minimum operating time to produce and extract, in situ, a high-quality section for TEM analysis.

The FIB-SEM is unlikely to replace Ar-ion milling in the near future, and the reasons for this, along with some practical considerations are worth a brief note. The FIB-SEM can be prohibitively expensive as it is currently two orders of magnitude more costly than a conventional ion mill. Also, the FIB-SEM requires several square meters of dedicated floor space, whereas an ion mill can be conveniently placed on a bench top. However, the most useful reason for one not replacing the other is that each tool provides valuable and complementary capabilities to the planetary-materials laboratory. The FIB-SEM is ideally suited to targeting small (tens of microns) and specific ROIs, whereas the Ar-ion mill works well for thinning large (hundreds of microns to mm) areas. Moreover, there is potential in combining the two methods. The amorphous damage layer that is produced during FIB milling can be significantly reduced by post-FIB Ar-ion milling (e.g., Huang 2004). Such post-FIB processing shows promise for improving the quality of sections of planetary materials.

SUMMARY

In situ FIB-SEM lift-out using microtweezers is a powerful method for the preparation of site-specific thin sections for coordinated analyses of planetary materials. Although we have focused on TEM and SIMS analyses, the FIB-prepared sections are also amenable to other microanalytical techniques such as synchrotron X-ray transmission microscopy (Busemann et al. 2006b, 2007). We have demonstrated the applicability of the technique to chondritic meteorites and presolar grains, but in situ lift-out is

applicable to a wide range of materials. Indeed, these techniques are currently being applied to the preparation of cometary dust samples from the Stardust aerogel collector and associated foils (e.g., Graham et al. 2004) and will likely become essential capabilities for future studies in earth and planetary materials.

Acknowledgments–We are grateful to Jorgen Rasmussen for assistance with the lift-out technique and acknowledge U.S. Patents 6,927,400 and 6,995,380 awarded to him and Ascend Instruments, LLC for the end effector and sample manipulation system, respectively. Constructive criticism provided by Drs. T. Bernatowicz, A. Brearley, associate editor C. Floss, and an anonymous referee are appreciated. We thank Drs. Carleton Moore (Arizona State University), Michael Zolensky (JSC), and Timothy McCoy (National Museum of Natural History) for samples. Research supported in part by NASA Astrobiology, Cosmochemistry, and Sample Return Laboratory Instruments and Data Analysis (SRLIDAP) programs.

Editorial Handling—Dr. Christine Floss

REFERENCES

Amari S., Lewis R. S., and Anders E. 1994. Interstellar grains in meteorites: I. Isolation of SiC, graphite, and diamond; size distributions of SiC and graphite. *Geochimica et Cosmochimica Acta* 58:459–470.

Barber D. J. 1993. Radiation damage in ion-milled specimens: Characteristics, effects, and methods of damage limitation. *Ultramicroscopy* 52:101–125.

Barber D. J. 1999. Development of ion-beam milling as a major tool for electron microscopy. *Microscopy and Analysis* 36:5–8.

Benzerara K., Menguy N., Guyot F., Vanni C., and Gillet P. 2005. TEM study of a silicate-carbonate-microbe interface prepared by focused ion beam milling. *Geochimica et Cosmochimica Acta* 69:1413–1422.

Bernatowicz T. J., Akande O. W., Croat T. K., and Coswik R. 2005. Constraints on grain formation around carbon stars from laboratory studies of presolar graphite. *The Astrophysical Journal* 631:988–1000.

Brearley A. J., Hanowski N. P., and Whalen J. F. 1999. Fine-grained rims in CM carbonaceous chondrites: A comparison of rims in Murchison and ALH 81002 (abstract #1460). 30th Lunar and Planetary Science Conference. CD-ROM.

Brown P. G., Hildebrand A. R., Zolensky M. E., Grady M., Clayton R. N., Mayeda T. K., Tagliaferri W., Spalding R., MacRae N. D., Hoffman E. L., Mittlefehldt D. W., Wacker J. F., Bird J. A., Campbell M. D., Carpenter R., Gingerich H., Glatiotis M., Greiner E., Mazur M. J., McCausland P. J., Plotkin H., and Mazur T. R. 2000. The fall, recovery, orbit, and composition of the Tagish Lake meteorite: A new type of carbonaceous chondrite. *Science* 290:320–325.

Buseck P. R. and Hua X. 1993. Matrices of carbonaceous chondrite meteorites. *Annual Review of Earth and Planetary Science* 21: 255–305.

Busemann H., Young A. F., Alexander C. M. O'D., Hoppe P., Mukhopadhyay S., and Nittler L. R. 2006a. Interstellar chemistry recorded in organic matter from primitive meteorites. *Science* 312:727–730.

Busemann H., Alexander C. M. O'D., Nittler L. R., Zega T. J., Stroud R. M., Cody G. D., Yabuta H., and Hoppe P. 2006b. Correlated microscale isotope and scanning transmission X-ray analyses of isotopically anomalous organic matter from the CR2 chondrite EET 92042 (abstract #2005). 37th Lunar and Planetary Science Conference. CD-ROM.

Busemann H., Zega T. J., Alexander C. M. O'D., Cody G. D., Kilcoyne A. L. D., Nittler L. R., Stroud R. M., and Yabuta H. 2007. Secondary ion mass spectrometry and X-ray absorption near-edge structure spectroscopy of isotopically anomalous organic matter from CR1 chondrite GRO 95577 (abstract #1884). 38th Lunar and Planetary Science Conference. CD-ROM.

Ciesla F. J., Lauretta D. S., Cohen B. A., and Hood L. L. 2003. A nebular origin for chondritic fine-grained phyllosilicates. *Science* 299:549–552.

Croat T. K., Stadermann F. J., and Bernatowicz T. J. 2005. Presolar graphite from AGB stars: Microstructure and *s*-process enrichment. *The Astrophysical Journal* 631:976–987.

Dobrzhinetskaya L. F., Green H. W., Weschler M., Darus M., Wang Y. C., Massonne H. J., and Stockhert B. 2003. Focused ion beam technique and transmission electron microscope studies of microdiamonds from the Saxsonian Erzgebirge, Germany. *Earth and Planetary Science Letters* 210:399–410.

Fegley B. J. and Prinn R. G. 1989. Solar nebula chemistry: Implications for volatiles in the solar system. In *The formation and evolution of planetary systems*, edited by Weaver H. A. and Danly L. Cambridge: Cambridge University Press. pp. 171–211.

Floss C., Stadermann F. J., Bradley J., Dai Z. R., Bajt S., and Graham G. 2004. Carbon and nitrogen isotopic anomalies in an anhydrous interplanetary dust particle. *Science* 303:1355–1358.

Gianuzzi L. A., Drown J. L., Brown S. R., Irwin R. B., and Stevie F. A. 1997. Focused ion beam milling and micromanipulation lift-out for site specific cross-section TEM specimen preparation. Proceedings, Materials Research Society Symposium. pp. 19–27.

Gianuzzi L. A. and Stevie F. A., eds. 2005. *Introduction to focused ion beams: Instrumentation, theory, techniques, and practice*. New York: Springer. 357 p.

Grady M. M., Verchovsky A. B., Franchi I. A., Wright I. P., and Pillinger C. T. 2002. Light element geochemistry of the Tagish Lake CI2 chondrite: Comparison with CI1 and CM2 meteorites. *Meteoritics & Planetary Science* 37:713–735.

Graham G. A., Grant P. G., Chater R. J., Westphal A. J., Kearsley A. T., Snead C., Dominguez G., Butterworth A. L., McPhail D. S., Bench G., and Bradley J. P. 2004. Investigation of ion beam techniques for the analysis and exposure of particles encapsulated by silica aerogel: Applicability for Stardust. *Meteoritics & Planetary Science* 39:1461–1473.

Heaney P. J., Vicenzi E. P., Gianuzzi L. A., and Livi K. J. T. 2001. Focused ion beam milling: A method of site-specific sample preparation for microanalysis of Earth and planetary materials. *American Mineralogist* 86:1094–1099.

Hewins R. 1997. Chondrules. *Annual Review of Earth and Planetary Science* 25:61–83.

Hoppe P., Strebel R., Eberhardt P., Amari S., and Lewis R. S. 2000. Isotopic properties of silicon carbide X grains from the Murchison meteorite in the size range 0.5–1.5 μm. *Meteoritics & Planetary Science* 35:1157–1176.

Huang Z. 2004. Combining Ar ion milling with FIB lift-out techniques to prepare high quality site-specific TEM samples. *Journal of Microscopy* 215:219–223.

Kato N. I. 2004. Reducing focused ion beam damage to transmission electron microscopy samples. *Journal of Electron Microscopy* 53:451–458.

Keller L. P., Messenger S., Flynn G. J., Clemett S., Wirick S., and Jacobsen C. 2004. The nature of molecular cloud material in

interplanetary dust. *Geochimica et Cosmochimica Acta* 68:2577–2589.

Ko D. S., Park Y. M., Kim S. D., and Kim Y. W. 2007. Effective removal of Ga residue from focused ion beam using a plasma cleaner. *Ultramicroscopy* 107:368–373.

Lauretta D. S., Hua X., and Buseck P. R. 2000. Mineralogy of fine-grained rims in the ALH 81002 CM chondrite. *Geochimica et Cosmochimica Acta* 64:3263–3273.

Lee M. R., Bland P. A., and Graham G. 2003. Preparation of TEM samples by focused ion beam (FIB) techniques: Applications to the study of clays and phyllosilicates in meteorites. *Mineralogical Magazine* 67:581–592.

MacPherson G. J., Wark D. A., and Armstrong J. T. 1988. Primitive material surviving in chondrites: Refractory inclusions. In *Meteorites and the early solar system*, edited by Kerridge J. F. and Matthews M. S. Tucson, Arizona: The University of Arizona Press. pp. 746–807.

Messenger S. 2000. Identification of molecular cloud material in interplanetary dust particles. *Nature* 404:968–971.

Metzler K., Bischoff A., and Stöffler D. 1992. Accretionary dust mantles in CM chondrites: Evidence for solar nebula processes. *Geochimica et Cosmochimica Acta* 56:2873–2897.

Nittler L. R. 2003. Presolar stardust in meteorites: Recent advances and scientific frontiers. *Earth and Planetary Science Letters* 209: 259–273.

Nittler L. R. and Alexander C. M. O'D. 2003. Automated isotopic measurements of micron-sized dust: Application to meteoritic presolar silicon carbide. *Geochimica et Cosmochimica Acta* 67: 4961–4980.

Nittler L. R., Alexander C. M. O'D., Gao X., Walker R. M., and Zinner E. K. 1997. Stellar sapphires: The properties and origins of presolar Al_2O_3 in meteorites. *The Astrophysical Journal* 483: 475–495.

Nittler L. R., Alexander C. M. O'D., Stadermann F. J., and Zinner E. K. 2005. Presolar Al-, Ca-, and Ti-rich oxide grains in the Krymka meteorite (abstract #2200). 36th Lunar and Planetary Science Conference. CD-ROM.

Seydoux-Guillaume A. M., Goncalves P., Wirth R., and Deutsch A. 2003. Transmission electron microscope study of polyphase and discordant monazites: Site-specific specimen preparation using the focused ion beam technique. *Geology* 31:973–976.

Stroud R. M., Nittler L. R., and Alexander C. M. O'D. 2004a. Polymorphism in presolar Al_2O_3 grains from asymptotic giant branch stars. *Science* 305:1455–1457.

Stroud R. M., Nittler L. R., and Alexander C. M. O'D. 2006. Supernova nierite (α-Si_3N_4) from Murchison (abstract). *Meteoritics & Planetary Science* 41:A168.

Stroud R. M., Nittler L. R., Alexander C. M. O'D., Stadermann F. J., and Zinner E. K. 2005. Microstructure of a presolar hibonite grain (abstract). *Meteoritics & Planetary Science* 40:A148.

Stroud R. M., Nittler L. R., and Hoppe P. 2004b. Microstructures and isotopic composition of two SiC X grains (abstract). *Meteoritics & Planetary Science* 39:A101.

Wirth R. 2004. Focused ion beam (FIB): A novel technology for advanced application of micro- and nanoanalysis in geosciences and applied mineralogy. *European Journal of Mineralogy* 16: 863–876.

Zega T. J. and Buseck P. R. 2003. Fine-grained-rim mineralogy of the Cold Bokkeveld CM chondrite. *Geochimica et Cosmochimica Acta* 67:1711–1721.

Zega T. J., Garvie L. A. J., and Buseck P. R. 2003. Nanometer-scale measurements of iron oxidation states of cronstedtite from primitive meteorites. *American Mineralogist* 88:1169–1172.

Zega T. J., Garvie L. A. J., Dódony I., and Buseck P. R. 2004. Serpentine nanotubes in the Mighei CM chondrite. *Earth and Planetary Science Letters* 223:141–146.

Zega T. J., Garvie L. A. J., Dódony I., Friedrich H., Stroud R. M., and Buseck P. R. 2006a. Polyhedral serpentine grains in CM chondrites. *Meteoritics & Planetary Science* 41:681–688.

Zega T. J., Stroud R. M., Nittler L. R., Busemann H., and Alexander C. M. O'D. 2006b. Correlated analytical studies of organic material from the Tagish Lake carbonaceous chondrite (abstract #1444). 37th Lunar and Planetary Science Conference. CD-ROM.

Zolensky M., Barrett R., and Browning L. 1993. Mineralogy and composition of matrix and chondrule rims in carbonaceous chondrites. *Geochimica et Cosmochimica Acta* 57:3123–3148.

Zolensky M. and McSween H. Y., Jr. 1988. Aqueous alteration. In *Meteorites and the early solar system*, edited by Kerridge J. F. and Matthews M. S., Tucson, Arizona: The University of Arizona Press. pp. 115–143.